Adsorption, Isomerization, and Decomposition of HCN on Si(100)2 × 1: A Computational Study with a Double-Dimer Cluster Model

F. Bacalzo-Gladden, Xin Lu,† and M. C. Lin*

Department of Chemistry and Cherry L. Emerson Center for Scientific Computation, Emory University, Atlanta, Georgia 30322

Received: January 26, 2001; In Final Form: March 14, 2001

The adsorption, isomerization, and decomposition of HCN on Si(100)-2 × 1 surface have been investigated by means of a density functional theory calculation using a double-dimer cluster model. The results revealed that both HCN and its HNC isomer can be readily adsorbed on a Si−Si dimer either dissociatively or molecularly in an end-on and a side-on configuration. Side-on adsorption occurs by the cycloaddition of the C≡N group on to the Si−Si dimer, whereas dissociative adsorption gives rise to H(a) and CN(a) adspecies initially via the end-on configuration on the same dimer or across the two dimers. Adsorbate−adsorbate interactions and reactions have also been studied with two HCN molecules. For the end-on adsorption, the first HCN(a) exerts a significant effect on the adsorption geometry of the second HCN. In particular, a synergetic effect has been observed for the parallel adsorption of two HCNs with their C═N groups bridging across the two dimers. For the side-on adsorption, the adsorbate−adsorbate interaction is negligible with minor effects on the adsorption geometry. H-migration between the two neighboring, side-on HCN admolecules can occur readily, leading to the formation of HCNH(a) and NC(a) surface species. The calculated vibrational frequencies of the HCNH(a) and NC(a) adspecies are in good agreement with the experimental HREELS data of the HCN/Si(100) system.

Introduction

The interaction of CN-containing species with Si surfaces is practically relevant to the chemical vapor deposition (CVD) of $SiCN_x$ films which have been shown to exhibit crystalline texture.[1−3] The mechanism for the adsorption and reactions of CN-containing compounds (such as HCN and C_2N_2) with the single crystal surfaces of Si has been investigated recently in this laboratory to understand the chemistry of CN_x−Si interactions.[4−6]

Bu et al.[4] reported the adsorption and thermal reaction of HCN (DCN) on Si(100)-2 × 1 using ultraviolet photoelectron spectroscopy (UPS), X-ray photoelectron spectroscopy (XPS), and high-resolution electron energy loss spectroscopy (HREELS). At dosages greater than 4 langmuirs and lower surface temperatures (T_s = 100 K), HCN formed dimers and polymers on Si(100). After the sample was annealed to 220 K, CN and HCNH adspecies were identified. The former showed a peak at 263 meV attributable to the C≡N stretching vibration, while the latter exhibited peaks at 160, 368, and ∼400 meV for the HC═NH, CH, and NH stretching vibrations, respectively. The adsorbed CN, CN(a), appeared to undergo reorientation from the end-on to the side-on configuration when the sample was annealed at 560 K. Above 680 K, the dissociation of NH and C≡N bonds took place. After the surface was annealed to temperatures >820 K, silicon carbide and silicon nitride were produced following the decomposition of CH(a) and the desorption of H species.

Bu et al.[5] have also investigated the interaction of HCN (DCN) with Si(111)-7 × 7 and compared their results with those obtained from the Si(100)-2 × 1 surface study mentioned above. At 220 K, CN(a) in an end-on adsorption geometry was identified as the major species which survived up to 600 K. In contrast, the relative concentration of the HCNH species was lower than that on Si(100)-2 × 1, and no significant reorientation of CN(a) was noted below 600 K. The observed difference between the interaction of HCN with Si(111)-7 × 7 and with Si(100)-2 × 1 was attributed to the different topologies of the two surfaces.

Recently, we have carried out a series of quantum-chemical studies on the adsorption mechanisms of CO,[7,8] NH_3,[9,10] HN_3,[10] C_2H_2,[11] CH_3OH,[12] CH_2O,[12] and HCOOH[12] with the reconstructed Si(100)-2 × 1 surface using the density functional theory and the cluster models of the surface.[13−18] We have also extended our theoretical study to the adsorption, isomerization, and decomposition of the HCN molecule on the Si(100)-2 × 1 surface. The preliminary result of this work using a single-dimer Si_9H_{12} surface model has been published previously.[19] In the present paper, we report in detail the results obtained by employing a larger, double-dimer $Si_{15}H_{16}$ surface model, to compare the energetics for HCN/HNC adsorption and isomerization reactions predicted by the two surface models as well as to study the role of adsorbate−adsorbate interactions that may lead to the formation of HCNH adspecies observed experimentally.[4]

Computational Procedures

We have used a $Si_{15}H_{16}$ surface model to represent the reconstructed Si(100)-2 × 1 surface. Its top layer consists of two adjacent dimers in the same dimer row.[8,11,20] All calculations

* To whom correspondence should be addressed. E-mail: chemmcl@emory.edu.

† Permanent address: State Key Laboratory for Physical Chemistry of Solid Surface and Department of Chemistry, Xiamen University, Xiamen 361005, China.

10.1021/jp010304n CCC: $20.00
Published on Web 04/21/2001

TABLE 1: Bond Distances (Å) and Relative Energies[a] (kcal/mol) of the Single HCN → HNC Isomerization Intermediates and Transition States on $Si_{15}H_{16}$ Cluster Calculated at B3LYP/6-31G* Level

parameter	d-LM1	d-TS1	d-LM2	d-TS2	d-LM3	d-TS3	d-LM4	d-TS1′	d-LM2′	d-TS3′	d-LM3′
R(C−H)	1.073	1.076	1.099	1.321				1.333	(4.322)		
R(N−H)				1.206	1.024	1.018	1.002			1.127	(4.387)
R(C−N)	1.154	1.176	1.290	1.323	1.330	1.227	1.165	1.186	1.185	1.193	1.165
$R(Si_d-C)$		(3.071)	1.966	2.020	2.032	1.921	1.892			1.876	1.856
$R(Si_d-N)$	1.896	1.903	1.837	1.904	1.861	(2.571)		1.881	1.763		
$R(Si_d-H)$								(2.493)	1.491	(2.255)	1.490
$R(Si_d-Si_d)_1$	2.394	2.404	2.342	2.387	2.346	2.435	2.422	2.432	2.386	2.524	2.385
$R(Si_d-Si_d)_2$	2.275	2.266	2.251	2.249	2.256	2.257	2.273	2.258	2.244	2.262	2.220
$R(Si_d-Si_{sub})$	2.374	2.368	2.358	2.359	2.358	2.366	2.378	2.364	2.360	2.367	2.355
ΔE	−15.6	−6.4	−31.7	+43.3	+1.1	+12.0	−11.8	−1.0	−51.4	+1.3	−58.7

[a] $\Delta E = E(CO_2/Si_{15}H_{16}) - E(CO_2) - E(Si_{15}H_{16})$.

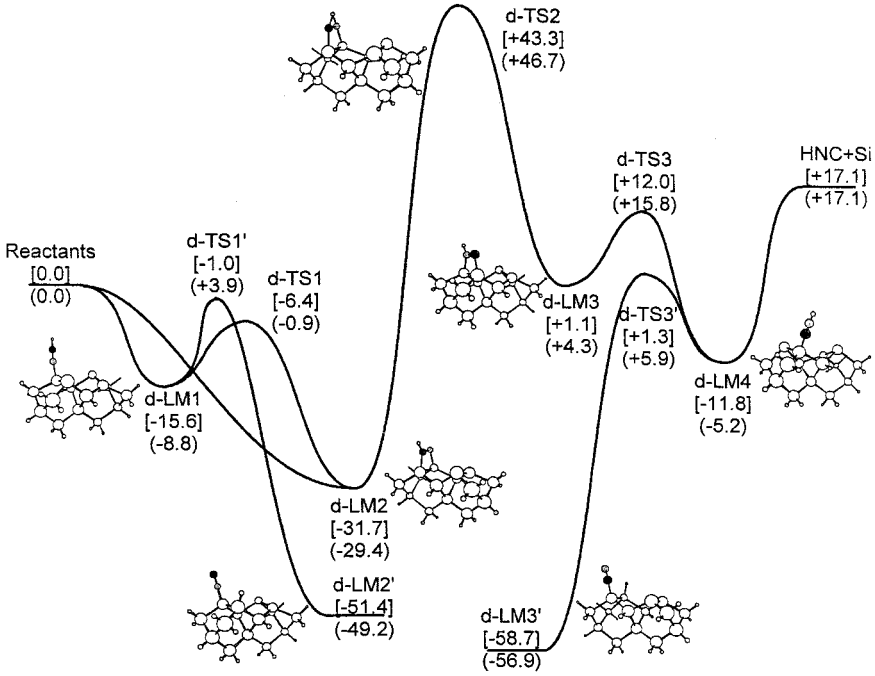

Figure 1. Potential energy surface of single HCN interacting with one of the dimers of the $Si_{15}H_{16}$ cluster calculated at the B3LYP/6-31G* level of theory. (Energies given in the square brackets were obtained using the $Si_{15}H_{16}$ cluster, while those in parentheses were obtained using the Si_9H_{12} cluster (ref 19)).

were performed with the GAUSSIAN 94 package.[21] The hybrid density functional method including Becke's 3-parameter nonlocal-exchange functional[22] with the correlation functional of Lee−Yang−Parr[23] (B3LYP) as well as analytical gradients was employed. The basis set used is the standard all-electron split-valence basis set 6-31G* including the polarization d-function on non-hydrogen atoms.[24] Geometry optimizations and vibrational analyses were performed without any constraint.

The results of the full geometry optimization calculations for the bare model surface gave the dimer separation, Si_d-Si_d (2.218 Å) and average subsurface bond distances, Si_d-Si_{sub} (2.347 Å) and $Si_{sub}-Si_{sub}$ (2.389 Å), which are in good agreement with those predicted for the smaller cluster models, Si_9H_{12} and $Si_{13}H_{20}$, as well as with experimental values.[7] Because of the size of the $Si_{15}H_{16}$ cluster model, final energies include the unscaled zero-point-energy (ZPE) corrections calculated at the B3LYP/LANL2DZ[25] level. Vibrational frequencies were also calculated at the B3LYP/LANL2DZ level.

Results and Discussion

1. Adsorption and Reactions of Single HCN Molecule. We first consider the adsorption and reaction of single HCN molecule on one of the two dimers of the $Si_{15}H_{16}$ cluster. The calculated geometrical parameters of the local minima and transition states are listed in Table 1 and the calculated energy profile is depicted in Figure 1. For comparison, the energetics obtained previously[19] with the Si_9H_{12} single-dimer cluster are also given (in parentheses) in Figure 1. As shown in Figure 1, the energy profile of the HCN isomerization and decomposition on the $Si_{15}H_{16}$ cluster is almost identical with that of HCN on the Si_9H_{12} cluster. The main features of HCN adsorption, isomerization, and decomposition on a Si−Si dimer can be summarized as follows.

(i) The end-on and side-on adsorption processes can proceed exothermically without barriers, leading to the formation of d-LM1 and d-LM2 adspecies, respectively. The formation of d-LM2 is predicted to be more exothermic by 16.1 kcal/mol than that of d-LM1. In the end-on mode, the HCN bonds to one surface Si atom with its 5σ molecular orbital (MO) lone pair donating charge into the empty, antibonding orbital of Si−Si dimer. The side-on adsorption, similar to the cycloaddition of acetylene onto the Si−Si dimer,[11,16,20,26] is simply a cycloaddtion of the -C≡N group onto the Si−Si dimer, leading to the formation of a closed, four-member ring surface species. The C≡N triple-bond in free HCN thus becomes C═N double-bond upon the side-on adsorption.

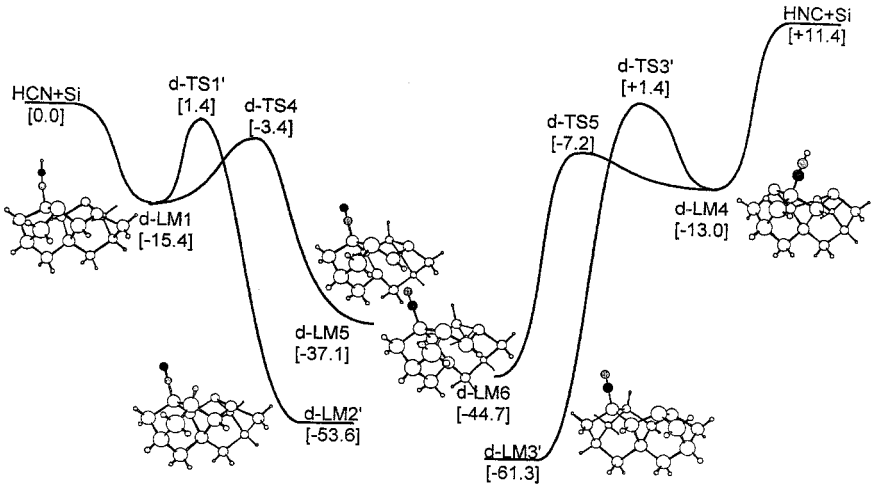

Figure 2. Potential energy surface for the dissociative adsorption of a single HCN(HNC) molecule over a single-dimer site and across two dimers calculated at the B3LYP/LANL2DZ level of theory.

(ii) d-LM1 can rearrange through a 9.2 kcal/mol barrier at d-TS1 and isomerize into the energetically more favorable d-LM2 in which the CN group is di-σ bonded with the two surface Si atoms within the same dimer.

(iii) Desorption of d-LM2 can be achieved either directly or indirectly by thermal activation from d-LM2 to d-LM1 with a barrier height of 25.3 kcal/mol.

(iv) Dissociative adsorption of HCN can proceed from d-LM1 via a transition state d-TS1′ with a barrier of 14.6 kcal/mol, giving rise to H- and CN-adspecies. Therefore, the end-on adsorption state is the precursor of the dissociative adsorption. The heat of dissociative adsorption is calculated to be −51.4 kcal/mol, indicating that the process is highly exothermic. Moreover, the transition state d-TS1′ is lower than the reactants by 1.0 kcal/mol, suggesting that the dissociative adsorption of HCN on the Si−Si dimer is feasible.

(v) So far as the HNC adsorbate is concerned, similar adspecies and transition states can be obtained as the HCN case. The corresponding adsorption configurations are d-LM4 (end-on adsorption), d-LM3 (side-on adsorption), and d-LM3′ (dissociative adsorption), with the transition state d-TS3 being responsible for the d-LM3 ⇔ d-LM4 rearrangement and the transition state d-TS3′ responsible for the dissociative adsorption process, d-LM4 ⇒ d-LM3′.

(vi) Furthermore, the di-σ bonded HCN (d-LM2) may undergo isomerization via d-TS2, with the H atom migrating from C to N producing the di-σ bonded HNC adsorbate, d-LM3. The barrier height of the isomerization process is calculated to be 75.0 kcal/mol above d-LM2, indicating it is practically insignificant to the HCN/Si chemistry.

From the energetics given in Figure 1, it can be seen that the energy difference between the single- and double-dimer cases, though nonnegligible, is consistent throughout the potential energy surface. On the average, the double-dimer configurations are more energetically favorable than their single-dimer counterparts by about 4 kcal/mol. This difference could be attributed to the cluster size and/or the surface effect of the second Si dimer, which lowers the total energy of the system. Furthermore, it is interesting to note that of all the intermediates, end-on adsorption is most affected by the double-dimer configuration, i.e., relative energies for d-LM1 and d-LM4 are lower by ∼6.7 kcal/mol as compared with the single-dimer cases. This reflects the greater stability of the side-on over the end-on adsorption due to di-σ bond formation in the former case.

We have also attempted to search for d-LM1 isomerization across the dimers in which C is coordinated with the third surface Si atom. Calculations at the B3LYP/6-31G* level for this type of configuration revealed an extreme buckling of the Si dimers resulting in severe surface reconstruction through which one of the surface Si atom is connected with a third-layer Si atom. The severe reconstruction may be an artifact of the limited size of cluster model employed. Note that the distance between two dimer rows is about 4.0 Å before adsorption and the C═N bond length in the side-on adsorbed HCN is as short as ∼1.3 Å (cf. Table 1). However, we cannot rule out the possibility of isomerization involving 2 HCNs across the dimers which we will explore in the next section.

We have also considered the possibility that HCN(HNC) may decompose across the two Si−Si dimers, i.e., HCN(HNC), dissociatively adsorbed onto the Si1 and Si3 sites. Once again, our B3LYP/6-31G* calculations for these dissociative adsorption processes revealed a similar severe surface reconstruction as that found for the isomerization of d-LM1 across the two dimers. However, no such reconstruction was found in the B3LYP/LANL2DZ calculations. The results reveal that dissociative chemisorption of HCN(HNC) takes place across the two dimers via a precursor state, d-LM1, and a transition state, d-TS4, giving rise to Si1-NC(-CN) and Si3-H surface species, as shown in Figure 2. The figure shows the potential energy surface for the dissociative chemisorption of one HCN(HNC) across the two dimers and over a single dimer calculated at the B3LYP/LANL2DZ level of theory. First, we should note that for the dissociative chemisorption over single dimer site, the B3LYP/LANL2DZ predicted energetics and geometry agree well with those predicted at the B3LYP/6-31G* level of theory. Second, it is interesting to find that the dissociative chemisorption across the two dimers has a lower barrier than that predicted for the dissociation over a single dimer. This suggests that the former pathway is kinetically more favorable than the latter pathway, despite the fact that the latter process is thermodynamically more favorable than the former one.

2. Adsorption and Reactions of Two HCN Molecules. *Adsorbate−Adsorbate Interactions.* Adsorption of a second HCN molecule on the double-dimer $Si_{15}H_{16}$ surface cluster is also investigated. Figure 3 shows the different possible adsorption configurations of two HCN molecules on the Si surface, while Table 2 lists their optimized geometric parameters and energies.

TABLE 2: Optimized Geometries (Å), Relative Energies[a] (kcal/mol), and Adsorption Energies[b] of the Second HCN Molecule Adsorbed on the Double Dimer Model

parameter	2LM1.d12	2LM1.d13	2LM1.d14	p-2LM2.d12	a-2LM2.d12	HCNH.d34	HCNH.ts1	HCNH.eb	HCNH.ts2
R(1C−1H)	1.074	1.072	1.099	1.099	1.099		1.236		1.591
R(1C−1N)	1.153	1.155	1.281	1.289	1.290	1.183	1.171	1.185	1.246
R(1Si_d−1C)			1.964	1.963	1.964				2.091
R(1Si_d−1N)	1.892	1.921	1.797	1.838	1.838	1.791	1.898	1.768	1.791
R(1Si_d−1Si_d)	2.396	2.372	2.408	2.347	2.346	2.411	2.390	2.405	2.438
R(2C−2H)	1.077	1.072	1.099	1.099	1.099	1.093	1.099	1.093	1.093
R(2N−2H)						1.024	1.495	1.023	1.189
R(2C−2N)	1.158	1.155	1.281	1.289	1.290	1.302	1.299	1.303	1.334
R(2Si_d−2C)			1.964	1.963	1.963	1.946	1.919	1.930	1.905
R(2Si_d−2N)		1.921	1.797	1.838	1.838	1.931	1.905	1.935	1.846
R(2Si_d−2H)	(3.099)								
R(2Si_d−2Si_d)	2.269	2.372	2.407	2.347	2.346	2.362	2.364	2.362	2.395
R(1Si_d−2Si_d)	3.974	3.944	3.168	4.006	3.985	3.872	3.968	3.318/3.672	3.199/3.276
$E_{rel.}$[a]	−21.9	−13.5	−95.3	−60.8	−61.5	−60.5	−31.2	−72.3	−32.7
$E_{ad}(2)$[b]	−6.3	(+2.1)		−29.1	−29.8				

[a] Energy with respect to 2E(HCN) + E($Si_{15}H_{16}$). [b] Adsorption energy of the second HCN molecule.

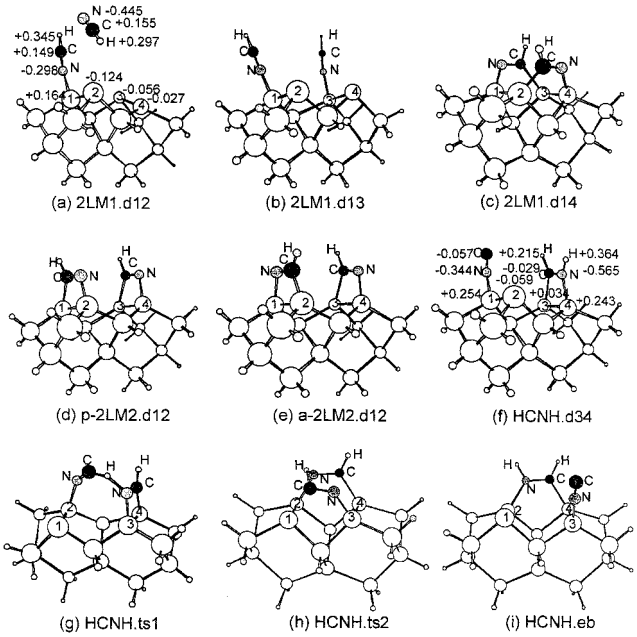

Figure 3. Geometries (a−i) of two HCN molecules adsorbed and reacted on the double-dimer cluster.

We have tested different geometries wherein two HCN could adsorb end-on onto the double-dimer cluster. First, both HCN molecules adsorb end-on the same surface Si dimer, 2LM1.d12. Second, one of the HCN molecules coordinates to an adjacent dimer, 2LM1.d13. Third, the second HCN molecule coordinates diagonally across form the first HCN molecule, 2LM1.d14. In the first case (see 2LM1.d12 in Figure 3a), we note that the second HCN molecule introduced onto the same dimer is just physisorbed on the Si surface with the second surface dimer almost unchanged (see also Table 2). The predicted adsorption energy for the physisorption of the second HCN is only −6.3 kcal/mol. It is clear that the presence of the first HCN molecule on the surface dimer prevents the second HCN molecule from chemisorbing onto the surface dimer. This is reasonable and easily predictable, as there is no suitable orbital on the Si−Si dimer to interact with the MOs of the second, incoming HCN after the empty, antibonding orbital of the dimer is being used to interact with the first HCN. The fact that the second HCN is inverted relative to the first HCN implies an electrostatic interaction between the two adsorbates.

Adsorption of two HCN molecules both in the end-on mode over the same side of adjacent dimers is shown in Figure 3b. The adsorption of the second HCN is predicted to be unfavorable with an endothermicity of 2.1 kcal/mol, and the Si−N bond length is elongated by about 0.03 Å upon the adsorption of the second HCN. The result suggests that the dipole−dipole interaction between the two adsorbates, which is always repulsive in nature, is substantial.

With regard to the third end-on adsorption geometry, 2LM1.d14, calculations at the B3LYP/6-31G* level indicate interestingly that both HCN molecules isomerize from an end-on to a side-on adsorption geometry in which the C atoms bond with the surface Si atoms across the dimers (see Figure 3c). The predicted total adsorption energy is −95.3 kcal/mol, showing the formation of such an adsorption configuration is highly exothermic and synergetic. Because of the short bond length of the CN groups that connect the two dimers, the dimer−dimer separation is severely shortened by 0.87 Å relative to a bare $Si_{15}H_{16}$ cluster (4.039 Å) with minimal relaxation of the Si_d-Si_{sub} bond distances. Interestingly, in our recent density functional study of the adsorption of acetylene on the Si(100)-2 × 1 surface,[11] a similar concerted adsorption configuration was also predicted with a high exothermicity.

Figure 3d and e shows the side-on adsorption on the same dimers with the two HCN parallel and antiparallel with each other, p-2LM2.d12 and a-2LM2.d12, respectively. The geometries of the two-adsorbate configurations are essentially the same as that of their one-adsorbate counterpart, d-LM2, with each CN group di-σ bonded on a Si−Si dimer. Both cases are predicted to have comparable stability. Particularly, the predicted adsorption energy of the second HCN (−29 kcal/mol) is lower by only 1.7 kcal/mol than that of the one-adsorbate case (−30.7 kcal/mol). This implies the presence of negligibly weak adsorbate−adsorbate repulsion in the two configurations. Accordingly, the adsorption of the second HCN in the side-on configuration shows minor effects on the adsorption geometry of the first side-on HCN adsorbate (see Tables 1 and 2).

Adsorbate−Adsorbate Reactions—Formation of HCNH Adspecies. Assuming that in the a-2LM2.d12 configuration H could migrate from one HCN adsorbate to another, we then obtained the HCNH(a) and CN(a) adspecies (see HCNH.d34 in Figure 3f). The HCNH adspecies is di-σ bonded onto one Si−Si dimer, while the CN-adspecies is singly bonded with its N-end on a Si atom of another Si−Si dimer. Both the HCNH.d34 and the a-2LM2.d12 configurations have comparable stability, with the latter one being thermodynamically favorable by only 1 kcal/mol over the former one. We have searched for the transition state of such a bimolecular surface reaction (see HCNH.ts1 in

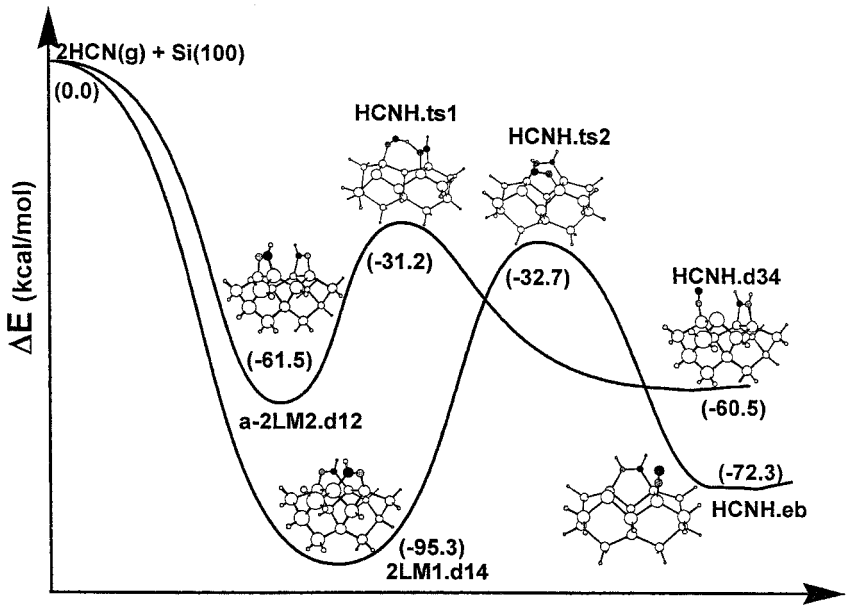

Figure 4. Two pathways for the formation of HCNH surfaces species from the bimolecular reaction of 2 HCNs on the Si(100)-2 × 1 surface predicted at the B3LYP/6-31G* level of theory.

Figure 3g) and found a barrier height of 30.3 kcal/mol with respect to the a-2LM2.d12 configuration. However, this transition state is lower than 2 free HCNs + $Si_{15}H_{16}$ by 31.2 kcal/mol. It means that the HCNH adspecies can be readily formed after the chemisorption of two HCNs onto the two neighboring Si−Si dimers.

We have further considered the possibility of HCNH(a) formation from 2LM1.d14 in which H-transfer is also likely to occur between the two HCN adsorbates. The geometry of the transition state, HCNH.ts2, of this H-transfer process is depicted in Figure 3h. The resultants are a CN(a) moiety singly bonded onto a Si atom and a HCNH(a) moiety side-on bonded over the end-bridge site of the two neighboring dimers. As such, the resultant configuration (see Figure 3i) is denoted as HCNH.eb. The formation energy of the HCNH.eb configuration is −72.3 kcal/mol with respect to free HCN and $Si_{15}H_{16}$, despite that it is less stable than the 2LM1.d14 configuration by 23 kcal/mol. The barrier height of this H-migration process is considerable with a predicted value of 62.6 kcal/mol due to the unexpectedly high stability of the 2LM1.d14 configuration. However, the result that the transition state, HCNH.ts2, is lower than the reactants, 2HCNs + $Si_{15}H_{16}$, by 32.7 kcal/mol suggests that the formation of HCNH adspecies from the 2LM1.d14 configuration is also feasible. The potential energy profiles for these two reaction pathways are presented in Figure 4.

Our finding that the HCNH adspecies can be readily formed upon H-transfer between two neighboring, side-on HCN adsorbates agrees with the experimental results of Bu and coworkers.[4] In their study on the HCN/Si(100)-2 × 1 system, they reported that after warming the 4-langmuir HCN dosed Si sample to 220 K (or <0.6 langmuir of HCN adsorbed on Si(100) at 100 K), two major adspecies, HCNH and CN, were found to be present on the surface based on their XPS, UPS, and HREELS results.[4]

3. Vibrational Frequencies of the HCNH(a) and NC(a) Species. The calculated vibrational frequencies of the HCNH and NC adspecies in the HCNH.d34 and HCNH.eb configurations are listed in Table 3, together with the experimental data extracted from the work of Bu et al.[4] In their HREELS experiments, they gave the following assignments, i.e., the peaks at 3428, 3226, 1613∼1290 cm^{-1} to N−H stretching, C−H stretching, and C═N stretching modes of the HCNH adspecies, respecitvely, and the peak around 2100 to N≡C stretching mode of the NC adspecies. Their assignments are now confirmed by our calculations on the HCNH.d34 and HCNH.eb configurations. Moreover, our calculations suggest that the N−H and C−H in-plane bending modes of the HCNH adspecies may contribute to the band ranging from 1290 to 1613 cm^{-1}.

TABLE 3: Comparison of Calculated HCNH Vibrational Frequencies (cm^{-1}) Using the Double Dimer (HCNH.d34) Models with Experiment[a]

mode	expt	HCNH.d34	HCNH.eb
HCNH(a) species			
N−H str	3428	3514	3500
C−H str	3226	3178	3154
C═N str	1290−1613	1498	1480
N−H, C−H bend (in-plane, asyn)		1401	1444
N−H, C−H bend (in-plane, syn)		1193	1269
N−H, C−H bend (out-of-plane, asyn)		1046	1053
N−H, C−H bend (out-of-plane, syn)		774	742
NC(a) species			
C≡N str	2097−2113	2089	2086

[a] Ref 4.

Concluding Remarks

The adsorption, isomerization, and decomposition of HCN on Si(100)-2 × 1 surface have been investigated by means of first-principles density functional cluster model calculations. For single molecule adsorption, the calculations revealed that (i) both HCN and its HNC isomer can be readily adsorbed on a Si−Si dimer either dissociatively or molecularly in an end-on mode and in a side-on mode; (ii) dissociative adsorption of HCN gives rise to H(a) and CN(a) adspecies, whereas dissociative adsorption of HNC results in H(a) and NC(a) adspecies; (iii) the side-on adsorption of HCN (or HNC) is reached by the cycloaddition of C≡N group onto a Si−Si dimer with the formation of a close, four-member ring (-Si−C═N−Si-) surface species.

Furthermore, adsorbate−adsorbate interactions and reactions have been studied by assuming two HCNs being adsorbed onto one Si−Si dimer or onto two neighboring Si−Si dimers. For two HCNs adsorbed on one Si−Si dimer, we found the second HCN can only be physisorbed. For the end-on adsorption on two dimers, the adsorbate−adsorbate interaction shows significant effects on the adsorption geometry. Particularly, a synergetic effect has been revealed when both HCN adsorbed in end-on mode onto two Si atoms of the two Si−Si dimers diagonally; the final adsorption geometry is that both HCNs with their C═N group bridge across the two dimers in a parallel manner. For the side-on adsorption, the adsorbate−adsorbate interaction was found to be negligible with minor effects on the adsorption geometry.

The mechanism for the formation of HCNH adspecies has been investigated. We found that H-migration between two neighboring side-on HCN admolecules can occur readily, leading to the formation of HCNH species which are also di-σ bonded. The calculated vibrational frequencies of the HCNH-(a) and CN(a) adspecies are in good agreement with the experimental HREELS data of the HCN/Si(100) system.

Acknowledgment. This work was sponsored by Emory University through the Robert W. Woodruff Professorship. One of us (X.L.) acknowledges a Visiting Fellowship from the Cherry L. Emerson Center for Scientific Computation.

References and Notes

(1) Chen, L. C.; Yang, C. Y.; Bhusari, D. M.; Chen, K. H.; Lin, M. C.; Lin, J. C.; Chuang, T. J. *Diamond Relat. Mater.* **1996**, *5*, 514.

(2) Bhusari, D. M.; Chen, C. K.; Chen, K. H.; Chuang, T. J.; Chen, L. C.; Lin, M. C. *J. Mater. Res.* **1997**, *12*, 1.

(3) Musin, R. N.; Musaev, D. G.; Lin, M. C. *J. Phys. Chem. B*, **1999**, *103*, 797, and references given therein.

(4) Bu, Y.; Ma, L.; Lin, M. C. *J. Phys. Chem.* **1993**, *97*, 7081.

(5) Bu, Y.; Ma, L.; Lin, M. C. *J. Phys. Chem.* **1993**, *97*, 11797.

(6) Bu, Y.; Ma, L.; Lin, M. C. *J. Phys. Chem.* **1995**, *99*, 1046.

(7) Bacalzo, F. T.; Musaev, D. G.; Lin, M. C. *J. Phys. Chem. B* **1998**, *102*, 2221.

(8) Bacalzo, F. T.; Lin, M. C. *J. Phys. Chem. B* **1999**, *103*, 7270.

(9) Lu, X.; Bacalzo F. T.; Lin, M. C., manuscript submitted for publication.

(10) Bacalzo-Gladden, F. T. PhD Dissertation, Emory University, May, 1999.

(11) Lu, X.; Lin, M. C. *Phys. Chem. Chem. Phys*. **2000**, *2*, 4213.

(12) Lu, X.; Zhang, Q.; Lin, M. C. *Phys. Chem. Chem. Phys*., in press.

(13) Redondo, A.; Goddard, W. A., III. *J. Vac. Sci. Technol*. **1982**, *21*, 344.

(14) Nachtigall, P.; Jordan, K. D.; Janda, K. C. *J. Chem. Phys.* **1991**, *95*, 8652.

(15) Wu, C. J.; Cater, E. A. *Phys. Rev. B.* **1992**, *45*, 9065.

(16) Liu, Q.; Hoffmann, R. *J. Am. Chem. Soc.* **1995**, *117*, 4083

(17) Konecný, R.; Doren, D. J. *J. Chem. Phys.* **1997**, *106*, 2426.

(18) Hu, D.; Ho, W.; Chen, X.; Goddard, W. A., III. *Phys. Rev. Lett.* **1997**, *78*, 1178.

(19) Bacalzo-Gladden, F.; Musaev, D. G., Lin, M. C. *J. Chin. Chem. Soc.-Taip*. **1999**, *46*, 395.

(20) Konecný, R.; Doren, D. J. *Surf. Sci*. **1998**, *417*, 169.

(21) Frisch, M. J.; Trucks, G. W.; Schlegel, H. B.; Gill, P. M. W.; Johnson, B. G.; Robb, M. A.; Cheeseman, J. R.; Keith, T.; Peterson, G. A.; Montgomery, J. A.; Raghavachari, K.; Al-Laham, M. A.; Zakrzewski, V. G.; Ortiz, J. V.; Foresman, J. B.; Peng, C. Y.; Ayala, P. Y.; Chen, W.; Wong, M. W.; Andres, J. L.; Replogle, E. S.; Gomperts, R.; Martin, R. L.; Fox, D. J.; Binkley, J. S.; Defrees, D. J.; Baker, J.; Stewart, J. P.; Head-Gordon, M.; Gonzalez, C.; Pople, J. A. *Gaussian 94*, *Revision B.3*, Gaussian, Inc., Pittsburgh, PA, 1995.

(22) Becke, A. D. *J. Chem. Phys.* **1993**, *98*, 5648.

(23) Lee, C.; Yang, W.; Parr, R. G. *Phys. Rev.* 1989, *B37*, 785.

(24) (a) Hariharan, P. C.; Pople, J. A. *Chem. Phys. Lett.* **1972**, *66*, 217, (b) Francl, M. M.; Pietro, W. J.; Hehre, W. J.; Binkley, J. S.; Gordon, M. S.; DeFrees, D. J.; Pople, J. A. *J. Chem. Phys.* **1982**, *77*, 3654.

(25) (a) Hay, P. J.; Wadt, W. R. *J. Chem. Phys.* **1985**, *82*, 270. (b) Wadt, W. R.; Hay, P. J. *J. Chem. Phys.* 1985, *82*, 284; (c) Hay, P. J.; Wadt, W. R. *J. Chem. Phys.* **1985**, *82*, 299.

(26) Imamura, Y.; Morikawa, Y.; Yamasaki, T.; Nakatsuji, H. *Surf. Sci. Lett*., **1995**, *341*, 1095.